

Proceeding to the LHC seminar talk *Update of the $B^0 \rightarrow K^{*0} \mu^+ \mu^-$ angular analysis at LHCb experiment* held by Eluned Smith on behalf of the LHC collaboration on 13th of March 2020.

Nils Breer

Technische Universität Dortmund

(das ist von fabian! nur als hilfe benutzen um zu wissen was da so rein kann.) The search for physics beyond the standard model continues especially in high precision measurements. One of the most promising decay types for new possible interactions are flavor changing neutral currents. In this analysis data from 2011, 2012 and 2016 is used to update the prior angular analysis of the process stated above which only used the 2011 and 2012 data. With twice the statistics and a better understanding of theoretical uncertainties the analysis confirms the local tension in P_5' found in the first analysis. A possible explanation of the tension is given by introducing a shift to the Wilson coefficient C_9 . This increases the significance of the tension to $2.7 - 3.3\sigma$.

The stated Process is of such importance because the $b \rightarrow s\mu\mu$ transition is forbidden at tree level due to FCNC and can only occur at loop order. Because of that, these processes are much more sensitive to new physics(NP).

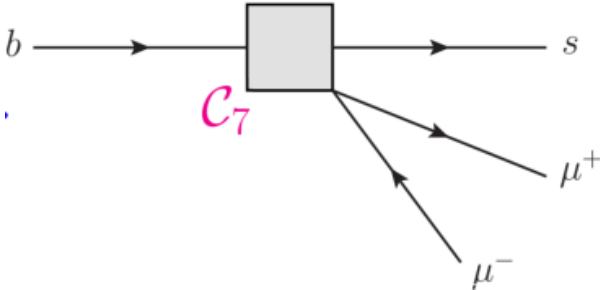


Figure 1: Wilson coefficient C_7 in .

To gather information about short distance NP above the SM energy scale μ , wilson coefficients $C_i(\mu)$ and low-energy QCD Operators O_i are used to describe that.

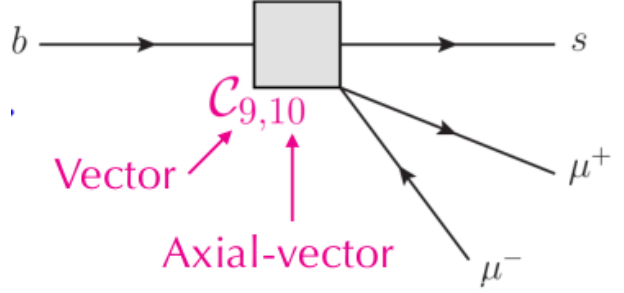


Figure 2: Process in new physics model.

The wilson coefficients C_7 , C_9 and C_{10} are of great importance since observables like the forward-backward asymmetry and P_5' are sensitive for C_9 especially.

In an effective theory, C_9 and C_{10} are used to describe the contribution from loops, in which electroweak gauge bosons are produced. wilson coefficient C_7 describes the contribution from loopdiagramms which produce photons from the loops.

This can be summarized by an effective hamiltonian

$$H_{eff} = -\frac{4G_f}{\sqrt{2}} V_{tb} V_{ts}^* \sum_i C_i \cdot O_i + \text{h.c.}$$

G_F is Fermi's constant, μ ist the renormalization scale, $V_{tb} V_{ts}^*$ is the contains leading flavor factors of the SM which lie in the CKM matrix elements V_{ij}

To measure the decay rate as a function of angles of the decay products, an angular analysis is performed. This is motivated by the fact, that the K^{0*} is a meson with spin 1 therefore three polarisation states. This results in a rich angular structure. The definition of the angular observables θ_k , θ_l and ϕ is schematically shown

in figure 3

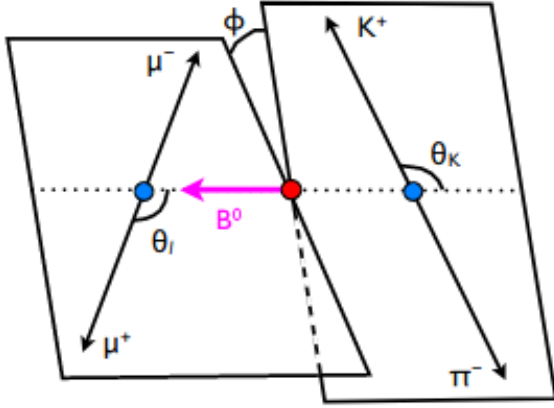


Figure 3: image of the angular observables.[3]

In this analysis, the forward-backard asymmetry A_{FB} , F_L the fraction of the longitudinal polarisation of the K^{*0} and the decay rate of the process $B^0 \rightarrow K^{*0} \mu \mu$ was measured. The definition of the angular observables are the following. θ_l is the angle between the negatively charged lepton and \bar{B} in the dimuon center of mass system (c.m.s). θ_k is the angle between the Kaon and the \bar{B} in the K^{*0} c.m.s.. The angle between the K^{*0} -plane and the dimuon-plane is defined by the angle ϕ [2].

Considering that S-wave contribution, spinless $K^+ \pi^-$ constellations, can pollute the measurement, therefore a parametrization such as $(1 - F_S)$ for this was taken into account where $(1 - F_S)$ is the S-wave fraction which describes the amount of S-wave contribution. The interference Amplitude between P-wave and S-wave decays are parametrized by A_S . The angular distribution[3] for the $B^0 \rightarrow K^{*0} \mu \mu$ decay reads

$$\frac{1}{\Gamma} \frac{d^3 \Gamma}{d\theta_k d\theta_l dq^2} = \frac{9}{16} f(F_S, A_S, \theta_k, \theta_l, A_{FB}, F_L)$$

Since A_{FB} , F_L and $\mathcal{A} \times E$ do not depend on the angle ϕ , it is already integrated out. The angular description for The B and \bar{B} are combined afterwards and expanded into a sum of the angular variables multiplied with a fitparameter, which are the A_{FB} , F_L and S_i 4, which are called CP-averaged observables because they contain CP violation.

Then the fit in the S_i basis was reparametrised to the P_i basis. This was done to eliminate first order uncertainties in the form factors primarily.

$$\frac{1}{d(\Gamma + \bar{\Gamma})/dq^2 d\cos\theta_l d\cos\theta_k d\phi} \bigg|_P = \frac{9}{32\pi} \left[\frac{3}{4} (1 - F_L) \sin^2 \theta_K + F_L \cos^2 \theta_K + \frac{1}{4} (1 - F_L) \sin^2 \theta_K \cos 2\theta_l - F_L \cos^2 \theta_K \cos 2\theta_l + S_3 \sin^2 \theta_K \sin^2 \theta_l \cos 2\phi + S_4 \sin 2\theta_K \sin 2\theta_l \cos \phi + S_5 \sin 2\theta_K \sin \theta_l \cos \phi + A_{FB} \sin^2 \theta_K \cos \theta_l + S_7 \sin 2\theta_K \sin \theta_l \sin \phi + S_8 \sin 2\theta_K \sin 2\theta_l \sin \phi + S_9 \sin^2 \theta_K \sin^2 \theta_l \sin 2\phi \right].$$

F_L : fraction of longitudinal polarisation of the K^{*0}

A_{FB} : forward-backard asymmetry of dimuon system

Figure 4: Angular description for B and \bar{B} combined.

The fit to the angular distribution yields seven CP violating observables including F_L . The P_i basis contains the amplitudes of the K^{*0} as angular coefficients as seen in table ??.

$$P_1 = \frac{2S_3}{1 - F_L} \quad P_{4,5,8}' = \frac{S_{4,5,8}}{\sqrt{F_L(1 - F_L)}} \\ P_2 = \frac{2}{3} \frac{A_{FB}}{1 - F_L} \quad P_6' = \frac{S_7}{\sqrt{F_L(1 - F_L)}} \\ P_3 = \frac{-S_9}{1 - F_L}$$

The angular distribution can be reduced to

$$\frac{1}{\Gamma} \frac{d^3 \Gamma[\bar{B}^0 \rightarrow \bar{K}^{*0} \mu^+ \mu^-]}{d\cos\theta_l d\cos\theta_k dq^2} = \frac{9}{16} \sum_i S_i(q_{min}^2, q_{max}^2) f_i(\vec{\Omega})$$

in the S_i basis. The S_i basis contains the six angular coefficients which are the combinations of the K^{*0} amplitudes and $\vec{\Omega} = (\cos\theta_l, \cos\theta_k)$. These amplitudes describe the polarization states of the Kaon.

This analysis especially focuses heavily on the tension induced by P_5' , since it is a very sensitive variable for C_9 . This can be seen in the range of 4 - 8 $\frac{\text{GeV}^2}{c^4}$ displayed in figure 5. The discrepancy is 2.8σ for the q^2 intervall from 4 - 6 $\frac{\text{GeV}^2}{c^4}$ and 3σ for the 6 - 8 $\frac{\text{GeV}^2}{c^4}$ intervall. For every collaboration a discrepancy between the SM and the measurement is visible, but the CMS measurement is the closest the the SM prediction.

For this analysis the data sets used are from the years 2011, 2012 and 2016. The data sets from 2011 and 2012 are from run 1. The 2011 data was taken at a centre of mass energy of $\sqrt{s} = 7 \text{ TeV}$, the 2012 data at $\sqrt{s} = 8 \text{ TeV}$ and the added data set from 2016 was taken at $\sqrt{s} = 13 \text{ TeV}$. Adding the 2016 data also doubled the statistic to around 4,7/fb.

For the selection of candidates it is required, that the impact paramters for the daughter par-

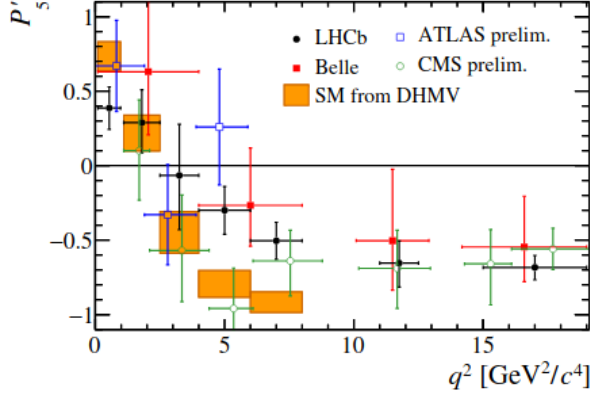


Figure 5: tension in P'_5 . [1]

ticles are quite significant since they do not originate from the primary vertex. Daughter particles that come from the primary need to have a very small impact parameter and also a quality vertex is necessary. That means the track fit $\frac{\chi^2}{dof}$ must be small, where dof are the degrees of freedom. To suppress peaking background as seen in figure 6 the particle identification is used. The FCNC process here is described by $B^0 \rightarrow K^{0*} \mu \mu$, but the subprocesses such as $B^0 \rightarrow K^{0*} (\bar{c}c \rightarrow \gamma^* \rightarrow \mu \mu)$ are statistically relevant since they proceed at tree level. Therefore charmonium resonances pollute the q^2 spectrum, especially at the $J/\Psi(1S)$ and the $\phi(2S)$ mass. Around these peaks a mass-veto region is defined where signal decays cannot occur. Left, in between and on the right of the peaks the signal regions are defined. A multivariate analysis (MVA) is performed to suppress combinatorial background even further. MVA is a machine learning technique in which a classifier or regressor takes several features to learn from and to make a prediction on what is background and what belongs to the signal. To suppress $J/\Psi \rightarrow l l$ contributions, the invariant mass spectrum is looked at. The most common features are: small momentum particles and small opening angles and a large dE/dx . Since the detector cannot know which lepton pairs belong together, all possible combinations are tested. Combinations with same signed leptons (N^{++} or N^{--}) are always uncorrelated so the signal S results in $S = N^{+-} - (N^{++} \text{ or } N^{--})$. This is called the like-sign method [4]. N^{+-} are the opposite sign lepton pairs.

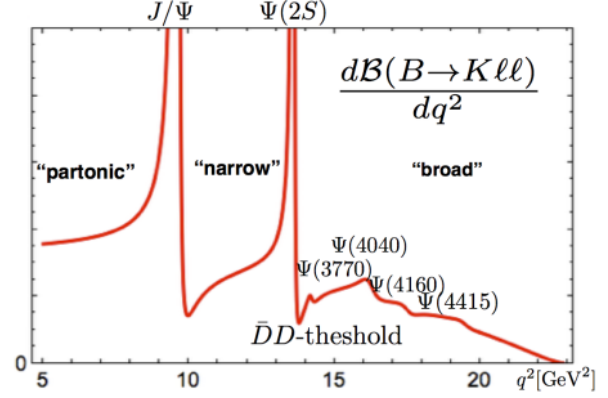


Figure 6: spectrum in q^2 for the lepton pair in $K ll$ branching fraction [1].

Now for the full fit model the shape of the invariant mass plots are used to determine the amount of signal and background in the data.

$$\text{PDF}_{total} = f_{sig} \text{PDF}_{sig}(\vec{\Omega}, m) + (1 - f_{sig}) \text{PDF}_{bkg}(\vec{\Omega}, m)$$

The PDF function can be separated into an angular part and a massive part. After that a maximum likelihood fit is performed. As seen in figure 7 the massive part of the signal PDF is a gaussian function with a radiative tail and the background PDF results in an exponential function.

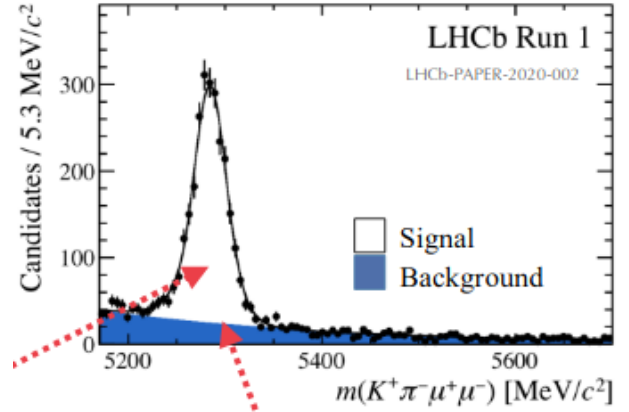


Figure 7: invariant B mass of Run 1 LHCb data.

Because of the factorization of the signal and background PDF

$$\text{PDF}_{sig}(\vec{\Omega}, m) = \text{PDF}_{sig}(\vec{\Omega}) \times \text{PDF}_{sig}(m)$$

$$\text{PDF}_{bkg}(\vec{\Omega}, m) = \text{PDF}_{bkg}(\vec{\Omega}) \times \text{PDF}_{bkg}(m)$$

the angular part of the signal PDF of the Run 1 data and the data from 2016 are shared

in the analysis to perform a simultaneous fit $\sum_i S_{i,q_{bin}^2} f_i(\Omega)$ because the angular part of the signal PDF corresponds to $f_i(\Omega)$. The S_i are thus used as fitparameters.

References

- [1] T. Blake et al. “Round table: Flavour anomalies in $b \rightarrow sl+l-$ processes.” In: *EPJ Web Conf.* 137 (2017). Ed. by Y. Foka, N. Brambilla, and V. Kovalenko, p. 01001. DOI: 10.1051/epjconf/201713701001. arXiv: 1703.10005 [hep-ph].
- [2] Christoph Bobeth, Gudrun Hiller, and Danny van Dyk. “The Benefits of $\bar{B} \rightarrow \bar{K}^* l^+ l^-$ Decays at Low Recoil.” In: *JHEP* 07 (2010), p. 098. DOI: 10.1007/JHEP07(2010)098. arXiv: 1006.5013 [hep-ph].
- [3] Serguei Chatrchyan et al. “Angular Analysis and Branching Fraction Measurement of the Decay $B^0 \rightarrow K^{*0} \mu^+ \mu^-$.” In: *Phys. Lett. B* 727 (2013), pp. 77–100. DOI: 10.1016/j.physletb.2013.10.017. arXiv: 1308.3409 [hep-ex].
- [4] Bjørn Bäuchle Stefan Kniege. *How to subtract combinatorial Background*. URL: https://fias.frankfurtium.de/downloads/04_hqm_cb.pdf (visited on 08/09/2020).